

Cite this: *Mater. Adv.*, 2022,  
3, 6791Received 15th May 2022,  
Accepted 18th July 2022

DOI: 10.1039/d2ma00544a

rsc.li/materials-advances

## Revisiting the origin of green emission in $\text{Cs}_4\text{PbBr}_6$

Koushik Biswas 

It is probably acceptable to state that the recent debate over the origin of green emission in  $\text{Cs}_4\text{PbBr}_6$  and/or  $\text{CsPbBr}_3$  has been narrowed down to two major possibilities: (i) a defect-mediated event in  $\text{Cs}_4\text{PbBr}_6$ , or (ii) a radiative recombination of charge carriers at  $\text{CsPbBr}_3$  inclusions embedded within  $\text{Cs}_4\text{PbBr}_6$ . The first scenario is relatively broad in terms of identifying specific defects that could act as recombination centers, although Br-vacancy has been proposed as a potential candidate. In the case of the second possibility, the omnipresence of  $\text{CsPbBr}_3$  nanoinclusions even in pure phase  $\text{Cs}_4\text{PbBr}_6$  is also a matter of contention. Resolving this “green emission question” is consequential to the further development of the Cs–Pb–X (X = halogen) system of perovskite-inspired optoelectronic materials. Here, we will briefly survey the current status of the literature and offer some perspectives with respect to the two possibilities noted above.

Perovskite halides, both hybrids (organic-inorganic) and all-inorganic, have been at the center of attention for over a decade due to their excellent optoelectronic properties. The surge in research activity among these ionic compounds has had at least two positive impacts. Continued progress in characterization and optimization has brought the leading perovskite candidates closer to commercialization, as is evident in the case of lead-halide perovskites reaching a power conversion efficiency of well over 20% for photovoltaic (PV) applications.<sup>1</sup> The other benefit is the proliferation of studies around halide materials that are promising in a number of applications including solar cells, light emitting diodes (LEDs) and scintillators.<sup>2,3</sup> In addition

to ease of synthesis and comprising of abundant constituents, some of these perovskites seem to defy the common understanding regarding the propensity of deep defects that would be detrimental to device applications. In contrast, they often exhibit excellent charge transport and light absorbing properties. These remarkable developments are opening new possibilities in a broad class of *perovskite-inspired* halides.

### Low-dimensional perovskites

Effective design principles are being implemented in the search for new perovskite-type compounds.<sup>4,5</sup> Fig. 1 shows such a concept where the 1-1-3 composition of the  $\text{A}^{\text{I}}\text{B}^{\text{II}}\text{X}_3$  halide ( $\text{A}^{\text{I}}$  = monovalent,  $\text{B}^{\text{II}}$  = divalent, X = halogen) transmutes to 0-dimensional (0D)  $\text{K}_2\text{PtCl}_6$ -type (2-1-6), 2-dimensional (2D) layered  $\text{Cs}_3\text{Fe}_2\text{Cl}_9$ -type or a 0D face sharing dimer phase (3-2-9), and 3-dimensional (3D) double perovskite structure (2-1-1-6) – all of which retain the  $[\text{BX}_6]$  octahedra in the crystal framework. Here, the dimensionality (*i.e.*, 0D, 2D, and 3D) refers to connectivity between the  $[\text{BX}_6]$  octahedra. For example, the 2-1-6 compounds feature isolated octahedra with A-ions filling the intervening voids. The 3-2-9 perovskite derivatives may appear in the 0D dimer phase or the layered 2D phase, as shown in Fig. 1. In general, the 2-1-6 and 3-2-9 compounds owing to their lower structural dimensionality lead to larger gap and poorer charge transport as compared to the state-of-the-art 3D perovskite  $\text{CH}_3\text{NH}_3\text{PbI}_3$ . This may be unfavorable for PV but does not preclude them as efficient light emitters, although multivalency of some constituent elements can induce harmful defect properties which may need to be addressed (*e.g.*, Sn changing its

Department of Chemistry and Physics, Arkansas State University, State University, Arkansas 72467, USA. E-mail: kbiswas@astate.edu



Koushik Biswas

*Koushik received his PhD in Physics from Texas Tech University (Lubbock, TX). After working as a postdoctoral associate at the National Renewable Energy Lab and Oak Ridge National Lab, he joined as a member of the faculty at Arkansas State University, Jonesboro. Here, he continues to work in the field of computational materials. His primary areas of interest include semiconductors and insulators in the field of optoelectronics.*



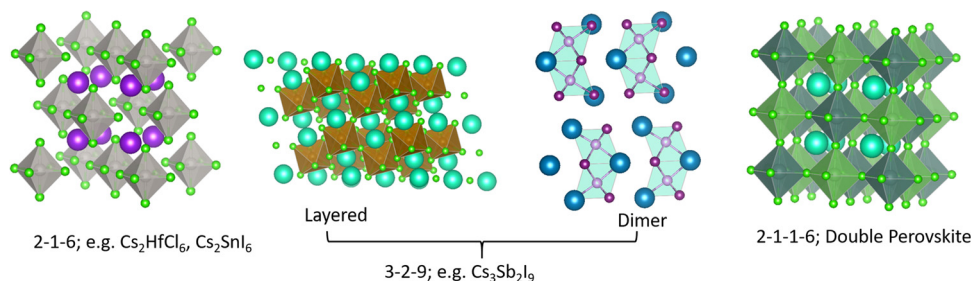


Fig. 1 Different structure types having chemical compositions 2-1-6, 3-2-9, 2-1-1-6; they may be termed as descendants from the  $A'B''X_3$  (1-1-3) perovskite family.

oxidation state from 4+ to 2+ and producing deep centers).<sup>6</sup> These examples demonstrate the versatility of crystal structures and chemical compositions available in the broad family of perovskites and perovskite derivatives, with tunable optoelectronic properties.

## The Cs–Pb–Br halides

The above discussion reminds us about the vast materials space offered by the perovskite-inspired halides that are waiting to be explored. Among these possibilities is the Cs–Pb–Br family comprising of  $CsPbBr_3$ ,  $CsPb_2Br_5$  and  $Cs_4PbBr_6$ .<sup>7–11</sup> Single crystals of  $CsPb_2Br_5$  have been recently reported.<sup>12</sup> It possesses a tetragonal lattice where Cs ions are sandwiched between  $Pb_2Br_5$  polyhedral layers. There are earlier reports of similar compounds with formula-type  $AB_2X_5$ , where the A and B sites are occupied by alkali, alkaline-earth or  $ns^2$  ions, and X = Cl, Br, or I. Based on relative ionic size ratio, it has been found that the tetragonal structure is usually favored when an  $ns^2$  ion (e.g.,  $Pb^{2+}$ ) occupies the ‘B’ site, as in the case of  $CsPb_2Br_5$ .<sup>13,14</sup> Several of these  $AB_2X_5$  compounds may be important optoelectronic materials, especially as scintillators.<sup>15</sup> In the following text, however, we focus on the ternary  $CsPbBr_3$  and  $Cs_4PbBr_6$  who are at the center of much debate on the subject of green emission.

$CsPbBr_3$  is already promising as a semiconductor radiation detector material.<sup>16</sup> Its iodide counterpart, *i.e.*,  $CsPbI_3$  has been reported as an all-inorganic candidate for efficient solar cells.<sup>17,18</sup> Both,  $CsPbBr_3$  and  $Cs_4PbBr_6$  feature the quintessential  $[PbBr_6]$  octahedra, with Cs ions occupying interstitial positions or voids created between those octahedra. But there is an essential difference between the two with respect to octahedral connectivity. At room temperature,  $CsPbBr_3$  crystals adopt an orthorhombic structure displaying a continuous network of corner-sharing octahedra, and are popularly described as a 3D halide perovskite.<sup>19,20</sup> On the other hand, the structure of  $Cs_4PbBr_6$  comprises of isolated octahedra with little wavefunction overlap and therefore referred as a 0D halide.<sup>21,22</sup> This structural difference has important consequences on their respective band structure and associated optoelectronic properties. Electronic structure calculations have shown the dispersive band edges of  $CsPbBr_3$  with a band gap  $\sim 2.3$  eV, whereas  $Cs_4PbBr_6$  expectedly has flat bands and a larger fundamental

gap of  $\sim 3.9$  eV.<sup>23,24</sup> Experimental band gaps roughly agree with these values.<sup>25–27</sup> Luminescence from  $CsPbBr_3$  single crystals is weak due to shallow excitons that are easily ionized to free carriers and energy transport is expected to be limited by shallow or deep traps. In  $Cs_4PbBr_6$ , however, the flat conduction and valence bands raise the opportunity for carriers to self-trap, and if they survive at room temperature, then charge transport and recombination may be dominated by polarons or excitons. Within this context we arrive at the dispute surrounding fast, green emission observed in  $Cs_4PbBr_6$  and/or  $CsPbBr_3$  samples approximately in the range 520–540 nm. Hereinafter, we refer to it as  $\sim 520$  nm emission. Notwithstanding the apparent agreement between emission wavelength and band gap of  $CsPbBr_3$ , the origin of luminescence could be a complex affair. Although it is a point of disagreement, recent reports seem to have narrowed it down to two main possibilities. Acknowledging the significant volume of the recent literature on this specific issue, we briefly explore a few around these two possibilities.

## Embedded $CsPbBr_3$ inclusions

Over the past several years, evidence has been gathering in favor of  $CsPbBr_3$  inclusions embedded in large-gap  $Cs_4PbBr_6$  as the source of green emission.  $Cs_4PbBr_6$  has a tendency to have impurity-phase  $CsPbBr_3$  due to incongruent melting, as noted initially by Nikl *et al.*<sup>25</sup> After presenting evidence of phase coexistence, they attributed the observed  $\sim 545$  nm emission to traces of  $CsPbBr_3$  in melt-grown  $Cs_4PbBr_6$  bulk crystals and thin films. Several recent reports have discussed the solution synthesis of emissive and non-emissive  $Cs_4PbBr_6$  bulk crystals, powders, films and nanocrystals (NCs).<sup>26,28–34</sup> Here, ‘emissive’ represents green luminescence. If we consider that luminescence is weak from  $CsPbBr_3$  single crystals at room temperature, but  $CsPbBr_3$  NCs have strong green photoluminescence (PL) quantum yield, then one could infer that emissive  $Cs_4PbBr_6$  possibly contains  $CsPbBr_3$  impurities.<sup>25,35</sup> Indeed, Akkermann *et al.* found that  $Cs_4PbBr_6$  films doped with 2%  $CsPbBr_3$  exhibited green PL similar to  $CsPbBr_3$  NCs, while pure  $Cs_4PbBr_6$  NCs and films did not.<sup>28</sup> It is notable that the 2% ‘doped’ sample produced similar X-ray diffraction (XRD) to the pure  $Cs_4PbBr_6$ . There are several reports on successful growth of non-emissive and green-emitting  $Cs_4PbBr_6$ .<sup>26,36–40</sup> Fig. 2 shows an example of  $Cs_4PbBr_6$  emissive and non-emissive nanocrystal suspension, while the larger



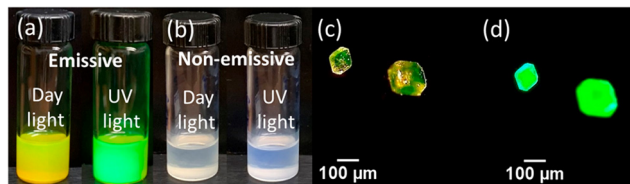


Fig. 2 Nanocrystal suspensions of (a) emissive and (b) non-emissive  $\text{Cs}_4\text{PbBr}_6$  under day light and UV exposure, respectively. Larger crystals of  $\text{Cs}_4\text{PbBr}_6$  under (c) white and (d) UV light. Reprinted (adapted) with permission from ref. 36. Copyright 2019 American Chemical Society.

crystals appear yellow under white light and bright green upon ultraviolet (UV) excitation.<sup>36</sup> Fig. 3a, as reported by Zhang *et al.*,<sup>26</sup> shows solution processed, millimeter-size transparent  $\text{Cs}_4\text{PbBr}_6$  crystals having no visible PL at room temperature and a broad UV peak around 370 nm. After vacuum annealing at 150 °C the crystals turned pale yellow and a bright green luminescence peak appeared around 525 nm as shown in Fig. 3b, similar to those shown in Fig. 2c and d. According to Zhang *et al.*,<sup>26</sup> a small absorption peak (not shown here) appearing at  $\sim 2.4$  eV in the yellow samples points towards the presence of  $\text{CsPbBr}_3$ .<sup>26</sup> Chen *et al.* mentioned that the initial nonstoichiometry induces the formation of  $\text{CsPbBr}_3$  nanocrystals in centimeter-sized crystalline  $\text{Cs}_4\text{PbBr}_6$  matrices.<sup>41</sup> There are many more experimental reports that indicate or support  $\text{CsPbBr}_3$  inclusions in  $\text{Cs}_4\text{PbBr}_6$ .<sup>42–50</sup>

Although these reports suggest the  $\text{CsPbBr}_3$  phase within  $\text{Cs}_4\text{PbBr}_6$ , complicating factors, namely, XRD and transmission electron microscopy (TEM) do not find evidence of  $\text{CsPbBr}_3$  and results are nearly identical in emissive *vs.* non-emissive samples.<sup>28,36,51,52</sup> This observation is not entirely unexpected due to the limitations of these techniques, failing to detect low concentrations of nanometer sized  $\text{CsPbBr}_3$  islands.<sup>36,50</sup> While XRD and TEM do not reveal any signature of  $\text{CsPbBr}_3$ , Raman spectroscopy data suggested otherwise as discussed by Qin *et al.*<sup>36</sup> A Raman active mode at  $\sim 29$   $\text{cm}^{-1}$  in emissive  $\text{Cs}_4\text{PbBr}_6$  coincided with a doublet feature at 28–30  $\text{cm}^{-1}$  observed in  $\text{CsPbBr}_3$ .

This study also reported on the pressure dependent evolution of Raman peaks and green PL intensity in emissive  $\text{Cs}_4\text{PbBr}_6$ . First, they established a 310  $\text{cm}^{-1}$  Raman line as a spectral signature to identify  $\text{CsPbBr}_3$  in  $\text{Cs}_4\text{PbBr}_6$ . Under hydrostatic pressure, the green PL and the 310  $\text{cm}^{-1}$  line follow a similar trend – both disappear at  $\sim 2$  GPa; thus offering some convincing data in favor of  $\text{CsPbBr}_3$  NCs as the source of  $\sim 520$  nm emission. Further evidence is provided by Riesen *et al.* who reported cathodoluminescence (CL) imaging with better spatial resolution of highly bright spots with wavelengths ranging between 500 and 540 nm that appeared in the  $\text{Cs}_4\text{PbBr}_6$  aggregate.<sup>53</sup> The similarity of the CL spectrum of the bright spots with the  $\text{CsPbBr}_3$  PL spectra corroborates their presence in the form of inclusions within  $\text{Cs}_4\text{PbBr}_6$ .

The work by Shin *et al.* also concluded that the origin of sub-bandgap luminescence in  $\text{Cs}_4\text{PbBr}_6$  films was due to residual  $\text{CsPbBr}_3$ .<sup>54</sup> The 3.9 eV absorption edge in these films are attributed to excitons. Thereafter, the excitons are confined in the lower gap  $\text{CsPbBr}_3$ , resulting in PL at 2.4 eV. The “emitter-in-matrix” design principle by Cao *et al.* provides additional impetus to the  $\text{CsPbBr}_3$  inclusion hypothesis.<sup>55</sup> They adopted this concept to describe the scintillation properties of  $\text{CsPbBr}_3$  NCs embedded inside the  $\text{Cs}_4\text{PbBr}_6$  host, demonstrating the superior performance of  $\text{CsPbBr}_3$ @ $\text{Cs}_4\text{PbBr}_6$  thin films for X-ray imaging applications.

Petralanda *et al.* implemented *ab initio* molecular dynamics, offering additional arguments in favor of the  $\text{CsPbBr}_3$  inclusion hypothesis.<sup>56</sup> By monitoring the time evolution of the ground (singlet) and excited (triplet) states as a function of temperature they found clear signatures of exciton–phonon coupling with increasing temperature. Hence, according to them, a mechanism for thermal quenching of excitonic emission exists in 0D  $\text{Cs}_4\text{PbBr}_6$ . Incidentally, thermal quenching of  $\text{Cs}_4\text{PbBr}_6$  emission has been reported in the experimental literature.<sup>25</sup> Computational work by Kang *et al.* revealed possible excitonic structures in  $\text{Cs}_4\text{PbBr}_6$  with emission in the UV range ( $\sim 387$  nm), whereas

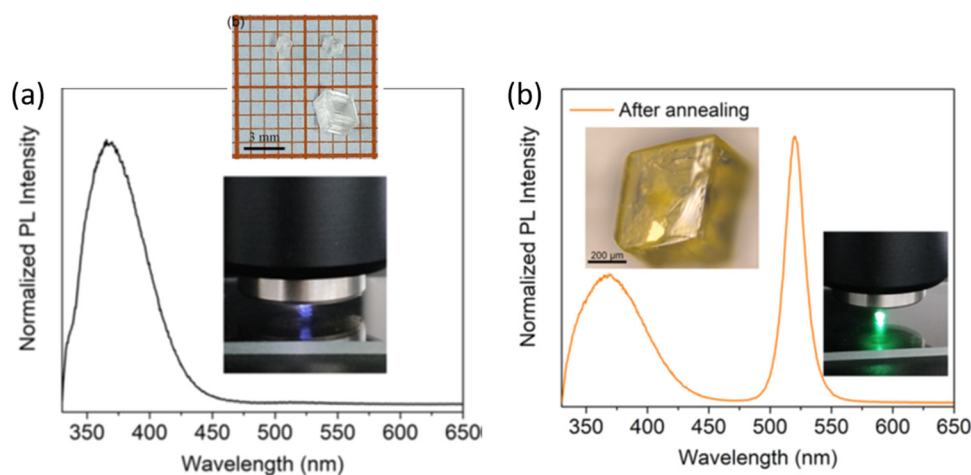


Fig. 3 (a) PL spectrum of as-grown  $\text{Cs}_4\text{PbBr}_6$  crystals showing no green luminescence (inset: photo of the transparent crystals and during PL using 325 nm excitation). (b) PL of the pale yellow samples obtained after annealing the crystals, with green luminescence around  $\sim 520$  nm. Reprinted (adapted) with permission from ref. 26. Copyright 2018 American Chemical Society.



similar triplet structures, meaning strongly bound excitons, could not be stabilized in the 3D CsPbBr<sub>3</sub>.<sup>23</sup> Those calculations did not reveal any Cs<sub>4</sub>PbBr<sub>6</sub> excitons that emit in the green. We should also note that transitions from purely triplet to singlet states are forbidden and therefore expected to be slow which goes against the observed fast green PL. According to calculations, possible type-I band alignment in concert with radiative or nonradiative energy transfer would favor the collection and concentration of carriers into the CsPbBr<sub>3</sub> recombination islands, thus favoring the concept of luminescence at CsPbBr<sub>3</sub> inclusions in the Cs<sub>4</sub>PbBr<sub>6</sub> host.<sup>23,57</sup>

Aside from CsPbBr<sub>3</sub> inclusions, other compositions have been proposed as a potential source of ~520 nm emission. For instance, Ray *et al.* discussed the presence of Cs<sub>2</sub>PbBr<sub>4</sub> inclusions alongside CsPbBr<sub>3</sub>.<sup>37</sup> Interestingly, Sun *et al.* also proposed the emergence of a 2D phase, Cs<sub>n+1</sub>Pb<sub>n</sub>Br<sub>3n+1</sub>, as emitting centers during the crystallization stage of Cs<sub>4</sub>PbBr<sub>6</sub>.<sup>58</sup> At  $n = 1$ , the 2D phase should be Cs<sub>2</sub>PbBr<sub>4</sub>, which is predicted to be direct gap, ~2.29 eV, and therefore a credible source of green emission.<sup>37,59</sup>

## Br-Vacancy or similar defects

Another strong hypothesis regarding green emission in pure phase Cs<sub>4</sub>PbBr<sub>6</sub> suggests a defect-mediated mechanism.<sup>38,51,60–68</sup> Bastiani *et al.* proffered the existence of intrinsic green luminescence centers, likely Br-vacancy (V<sub>Br</sub>).<sup>69</sup> Their Cs<sub>4</sub>PbBr<sub>6</sub> crystals had a pale green color under ambient light and appeared bright green when exposed to 365 nm UV radiation. Utilizing temperature dependent PL, they showed rapid quenching of PL intensity that was reversible up to about 180 °C and became irreversible above that temperature. This observation coupled with their temperature dependent XRD, which showed the appearance of CsPbBr<sub>3</sub> peaks at elevated temperatures led them to conclude that formation of CsPbBr<sub>3</sub> phase may actually oppose green emission instead of enabling it. The authors of ref. 69 also reported similar electron diffraction patterns of emissive and non-emissive Cs<sub>2</sub>PbBr<sub>4</sub> with no reflection that could be ascribed to CsPbBr<sub>3</sub> in either sample. We remind our readers that emissive in this case refers to green luminescence. Altogether, they found that green emission in Cs<sub>4</sub>PbBr<sub>6</sub> is independent of CsPbBr<sub>3</sub> which points to the possibility of an intrinsic defect center that produces gap states where radiative recombination can occur. Since halogen vacancies are expected to be abundant and often create sub-gap states in insulating halides, V<sub>Br</sub> in Cs<sub>4</sub>PbBr<sub>6</sub> was proposed as a possible candidate.<sup>29,69</sup> These reports were followed by those of Yin *et al.* who performed a comprehensive study of native defects in CsPbBr<sub>3</sub>, Cs<sub>2</sub>PbBr<sub>5</sub>, and Cs<sub>4</sub>PbBr<sub>6</sub> using density functional theory (DFT).<sup>24</sup> According to their calculations, V<sub>Br</sub> is shallow in the former two compounds, but it is a deep defect in Cs<sub>4</sub>PbBr<sub>6</sub> with a +/0 transition level ~2.3 eV above the valence band maximum (VBM). Several more native defects produced deep midgap states in Cs<sub>4</sub>PbBr<sub>6</sub>. Nevertheless, V<sub>Br</sub> appeared to be the most likely candidate due to its low formation energy under Br-poor conditions. It is important to note that this study,<sup>24</sup> and

previous works by the same group have reported on the phase purity of experimentally grown emissive samples of Cs<sub>4</sub>PbBr<sub>6</sub> with no traces of CsPbBr<sub>3</sub>. It conflicts with other groups' claim of phase coexistence in Cs<sub>4</sub>PbBr<sub>6</sub>.<sup>36,37,50,53,58</sup>

Based on a detailed analysis of femtosecond transient absorption spectroscopy Liu *et al.* attributed green luminescence in Cs<sub>4</sub>PbBr<sub>6</sub> single crystals to exciton migration to a defect level occurring within several hundred femtoseconds, followed by exciton relaxation and recombination in the picosecond and the subnanosecond or nanosecond time scale, respectively.<sup>70</sup> Chen *et al.* inferred a similar mechanism where excitons are trapped potentially at halogen related defect states in Cs<sub>4</sub>PbBr<sub>6</sub> which then recombine to generate the observed luminescence.<sup>64</sup>

Recently, Cha *et al.* investigated the magnetic properties of Cs<sub>4</sub>PbBr<sub>6</sub> that provide new insights into this issue.<sup>40</sup> Single crystals were found to have paramagnetic components in emissive Cs<sub>4</sub>PbBr<sub>6</sub>, while the non-emissive crystals exhibited exclusively diamagnetic behavior. This notable difference in magnetic response of the emissive crystals is due to V<sub>Br</sub> which serve as paramagnetic domains and green emission centers.

Studies reported by Yang *et al.* also support the defect mechanism, but offer yet another reason for green emission.<sup>71</sup> In this case, Cs<sub>4</sub>PbBr<sub>6</sub> micro-particles were synthesized involving ethanol as a polar solvent. Assisted by DFT calculations, they infer that the impact of the OH- group (presumably from ethanol) was to reduce the band gap of the Cs<sub>4</sub>PbBr<sub>6</sub> host from 3.75 eV to 3.5 eV, also downshifting the Br-vacancy level from 2.75 eV to 2.44 eV, which approximately matches with the ~520 nm green emission. In another report, Hu *et al.* found that interstitial hydroxyl induces a calculated sub-gap level at 2.6 eV and is therefore a possible reason for green PL.<sup>72</sup> Similar effects of hydroxyl level inside Cs<sub>4</sub>PbBr<sub>6</sub> have been reported.<sup>73</sup>

Using first-principles theory Jung *et al.* reported several uncharacteristic findings about the nature of point defects in Cs<sub>4</sub>PbBr<sub>6</sub>.<sup>74</sup> The calculated equilibrium chemical potential diagram shown in Fig. 4 verifies the narrow (shaded) region of stability of Cs<sub>4</sub>PbBr<sub>6</sub>, bound by the competing binary and ternary phases. Three points marked A, B, and C in the stable region of Cs<sub>4</sub>PbBr<sub>6</sub> perhaps correspond to Br-rich, stoichiometric (*i.e.*, neither rich nor poor), and Pb-rich conditions, respectively. The defect formation energies of various native defects corresponding to points A, B and C are also shown in Fig. 4. According to this report,<sup>74</sup> most native defects are deep with heavy compensation among the positive and negative charged defects and low equilibrium carrier concentrations of less than 10<sup>9</sup> cm<sup>-3</sup>. Their contention that the V<sub>Br</sub> concentration will remain low conflicts with the low formation energy (hence, high concentration) under Br-poor conditions reported by Yin *et al.*<sup>24</sup> Based on an analysis of the configuration coordinate diagram of several prominent defects including V<sub>Br</sub>, Jung *et al.* ruled out the possibility of visible emission except for the curious case of the Br<sub>Cs</sub> (Br at Cs site) defect. A closer inspection of this defect revealed that the antisite Br<sub>Cs</sub> actually bonds with two neighboring Br ions forming a Br<sub>3</sub> molecular species.



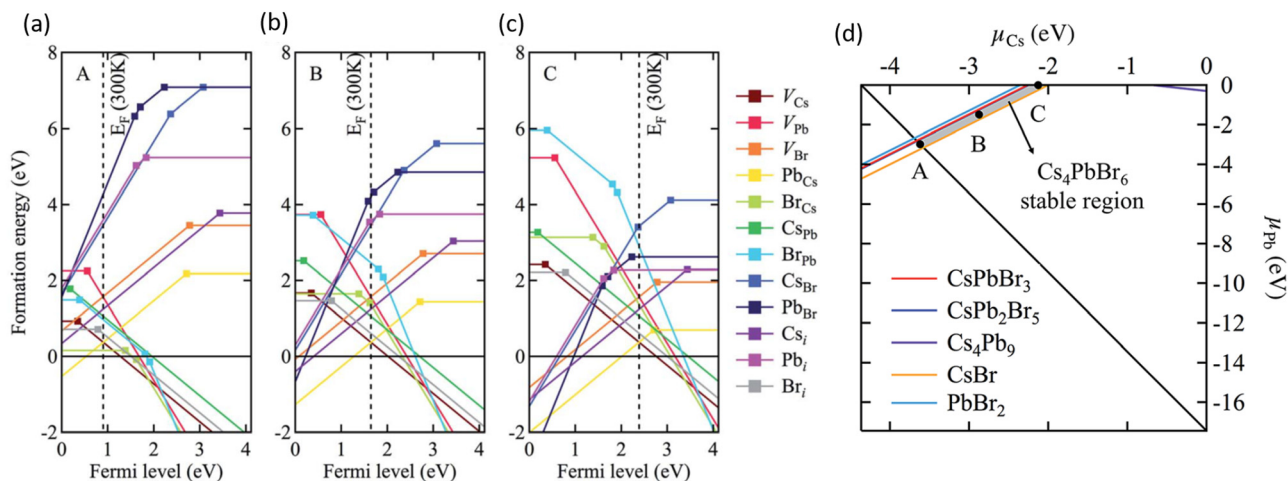


Fig. 4 (a–c) Calculated formation energy of native defects as a function of Fermi energy inside the band gap of Cs<sub>4</sub>PbBr<sub>6</sub>. The zero of energy is set at the VBM. The three figures correspond to points A, B and C shown in (d) which depicts the calculated ranges of chemical potentials of stable Cs<sub>4</sub>PbBr<sub>6</sub> under equilibrium. Reprinted (adapted) with permission from ref. 74. Copyright 2019 The Royal Society of Chemistry.

Furthermore, they suggested a radiative mechanism involving BR<sub>3</sub><sup>-</sup> that could result in green emission.<sup>74</sup>

## Concluding remarks

Looking back at the volume of scientific research dedicated to green PL in the ternary Cs–Pb–Br system, it is clear that strong arguments are presented by both sides. The case of extrinsic causes such as an impurity phase (or inclusions) is shown in Fig. 5a. It presents a plausible scenario where CsPbBr<sub>3</sub> inclusions appear within Cs<sub>4</sub>PbBr<sub>6</sub>, with type-I band edge alignment between the two phases. It facilitates the collection of excited charge carriers from Cs<sub>4</sub>PbBr<sub>6</sub> to CsPbBr<sub>3</sub> islands and subsequent recombination, producing an ~520 nm emission. This scenario is muddled by the reports of green-emitting Cs<sub>4</sub>PbBr<sub>6</sub> where XRD and high resolution TEM did not find any evidence of CsPbBr<sub>3</sub>. The PL properties of CsPbBr<sub>3</sub> and Cs<sub>4</sub>PbBr<sub>6</sub> are very similar, which only adds to the confusion. As already stated, there are also reports of emissive and non-emissive Cs<sub>4</sub>PbBr<sub>6</sub> with identical XRD patterns. In fact, the successful growth of

non-emissive Cs<sub>4</sub>PbBr<sub>6</sub> may be strong evidence in favor of the inclusion hypothesis. Even if CsPbBr<sub>3</sub> is present due to incongruent melting and the narrow region of stability of pure Cs<sub>4</sub>PbBr<sub>6</sub> (Fig. 4d), uniform fabrication techniques (across research groups) that are able to reproduce both emissive and non-emissive samples will go a long way towards resolving the role of CsPbBr<sub>3</sub>@Cs<sub>4</sub>PbBr<sub>6</sub> in the ~520 nm emission. Similarly, on the computational side, reports of type-I or type-II band alignment between Cs<sub>4</sub>PbBr<sub>6</sub> and CsPbBr<sub>3</sub> need to be clarified too.

There are additional issues regarding the Cs<sub>4</sub>PbBr<sub>6</sub>/CsPbBr<sub>3</sub> host-island interface that deserve careful consideration. For example, Ling *et al.* suggested shallow states created at the interface are responsible for the enhancement of green PL in the Cs<sub>4</sub>PbBr<sub>6</sub>/CsPbBr<sub>3</sub> composite.<sup>48</sup> Xu *et al.* proposed that the enhanced oscillator strength of imbedded CsPbBr<sub>3</sub> nanocrystals (relative to its extended crystal form) may be due to the lower dielectric constant of the surrounding Cs<sub>4</sub>PbBr<sub>6</sub> matrix, reminiscent of dielectric confinement.<sup>42</sup> According to reports, the static dielectric constant of Cs<sub>4</sub>PbBr<sub>6</sub> (~6 to 8) is indeed lower than CsPbBr<sub>3</sub> (~20).<sup>23,74,75</sup> It is important to determine whether the chemical correspondence between the host and island present a

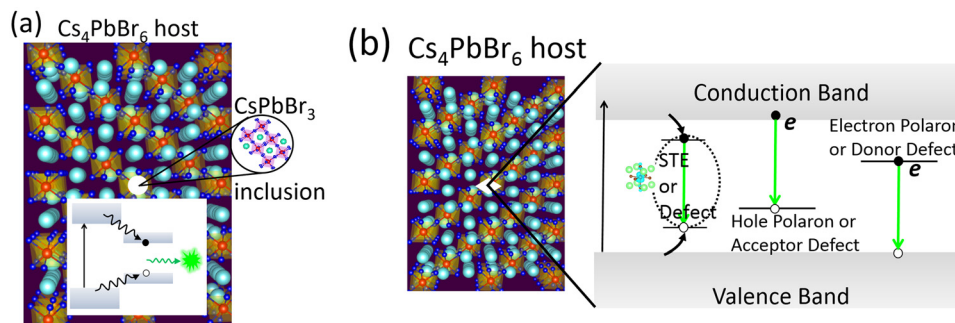


Fig. 5 (a) CsPbBr<sub>3</sub> emitters appearing as nano-inclusions within Cs<sub>4</sub>PbBr<sub>6</sub>. A type-I band alignment will favor the collection and subsequent recombination of charge carriers, producing green PL. (b) Possible optical transitions involving self-trapped excitons, (electron or hole) polarons, and defects inside the band gap of Cs<sub>4</sub>PbBr<sub>6</sub> as the source of green PL.



fortunate case where the aforementioned shallow states and dielectric confinement act in concert to aid stronger emission. Clarifying these aspects is essential to optimizing the PL properties by engineering the shape, size and distribution of emitting centers in a  $\text{Cs}_4\text{PbBr}_6$  matrix.

As a final remark, a recent work on ‘dots-in-a-matrix’ by Ning *et al.* demonstrated the successful solution growth of epitaxially aligned PbS quantum dots passivated inside  $\text{CH}_3\text{NH}_3\text{PbI}_3$  films, which they termed poly-heterocrystalline solids.<sup>76</sup> They found that the photogenerated carriers in the larger gap  $\text{CH}_3\text{NH}_3\text{PbI}_3$  matrix can be efficiently transferred to the smaller gap quantum dots for subsequent emission in the infrared region – thus leveraging the best features of both components. A similar situation is possible in the form of  $\text{CsPbBr}_3$  emitters in  $\text{Cs}_4\text{PbBr}_6$ , as schematically depicted in Fig. 5a. Indeed, the  $\text{CsPbBr}_3@/\text{Cs}_4\text{PbBr}_6$  scintillators by Cao *et al.*<sup>55</sup> is rooted in this principle. In the context of  $\text{CsPbBr}_3@/\text{Cs}_4\text{PbBr}_6$  scintillators, Prof. Williams and colleagues cautioned about some pitfalls when it comes to applying them as energy resolving radiation detectors, where light yield from bulk crystals is important.<sup>77</sup> Even if energy transfer is efficient from the  $\text{Cs}_4\text{PbBr}_6$  matrix to  $\text{CsPbBr}_3$  nanoinclusions (as in quantum dots in a matrix), a small Stokes shift could lead to the problem of self-absorption of the emitted light by  $\text{CsPbBr}_3$ . It may be severe when material thickness is required to be in the centimeter range to stop high energy ionizing radiation. This is why scintillators for spectroscopic  $\gamma$ -ray detection are either self-activated or doped with activator ions who provide the needed Stokes shift. The self-absorption problem is not a big limitation in the case of (nonspectroscopic) thin film applications for X-ray imaging or electroluminescent devices (LEDs, for example).

The defect-mediated green emission hypothesis in  $\text{Cs}_4\text{PbBr}_6$  also has its own set of unanswered questions and accompanying opportunities. Fig. 5b shows a schematic representation of potential optical transitions that could lead to  $\sim 520$  nm emission. It includes the case a self-trapped exciton, although no such signature has been detected theoretically or experimentally, thus far. Among the potential defects, whether it is  $V_{\text{Br}}$ ,  $\text{Br}_3$  or some other point defect, fast emission dictates efficient energy transfer at room temperature to the defect site for radiative recombination. Upon excitation, self-trapped excitons (STEs) are expected to form *via* electron–phonon coupling. However, the 375 nm STE emission band of  $\text{Cs}_4\text{PbBr}_6$  begins quenching at 100 K and becomes weak by 250 K.<sup>25,56</sup> Du *et al.* linked the quenching at higher temperature to the significant electronic coupling between  $[\text{PbBr}_6]$  octahedra and spectral overlap between STE absorption and emission (small Stokes shift). Accordingly, they suggest a mechanism of exciton migration *via* nonradiative resonant energy transfer between the  $[\text{PbBr}_6]$  octahedra, and increased chance of energy loss at lattice defects.<sup>75,78</sup>

It has been suggested that the appearance of an Urbach tail in the absorption spectrum of  $\text{Cs}_4\text{PbBr}_6$  is indicative of localized states in the gap. A rather large Urbach energy of about 1.7 eV has been estimated.<sup>51</sup> For argument’s sake, subtracting this value from the  $\text{Cs}_4\text{PbBr}_6$  band gap of  $\sim 3.9$  eV results in an energy close to the green luminescence. On the contrary,

Kajino *et al.* recently evaluated the Urbach energy of  $\text{CsPbBr}_3/\text{Cs}_4\text{PbBr}_6$  to be about 16.6 meV, dominated by phonon interactions.<sup>79</sup> Irrespective of its value, the contribution to the Urbach energy may come from any physically valid mechanism including electron–phonon interactions and defect states. While defect-trapped excitons are a possible route for exciton relaxation (and subsequent emission), an in-depth study will be necessary to justify defects as the primary cause of broadened absorption edge of  $\text{Cs}_4\text{PbBr}_6$ .<sup>80</sup>

Besides the need for energy transfer to a radiative center, nonradiative processes may be in competition, whose rate depends on the carrier capture cross-section of a charged or neutral defect and its ionization energy with respect to the conduction or valence band edge. The mere abundance of a defect at a deep level is not sufficient for optical transition at a specific wavelength. For instance, let us pick  $V_{\text{Br}}$  where there is agreement about its deep level inside the band gap of  $\text{Cs}_4\text{PbBr}_6$ . Its different charge states are positive where the defect level is empty ( $V_{\text{Br}}^+$  in semiconductor point defect nomenclature), neutral or singly occupied ( $V_{\text{Br}}^0$ ), and a fully occupied negative charge state ( $V_{\text{Br}}^-$ ). Note that the equilibrium defect levels corresponding to each of the charged states have different energetic positions because of differences in lattice relaxation and the energy cost of doing so. Therefore, defect induced single particle levels may or may not reside inside the band gap, although in this case it appears they are inside the gap. Regarding the question of photon emission involving these levels, it is possible either due to decay of an electron from the conduction band minimum (CBM) to an unoccupied state or due to recombination of an electron in the occupied defect state with a hole at the VBM (see Fig. 5b). The first transition communicates with electrons at the CBM while the latter with holes at the VBM. Theory and experimentation have not yet clarified which defect’s initial and final states could result in such a transition producing ultrafast green PL. It is not to say that defects in  $\text{Cs}_4\text{PbBr}_6$  is the unlikely cause, in fact, there are plenty of examples among scintillators where activators (dopants behaving like point defects) produce sub-band gap states for efficient and fast optical decay, as in  $\text{LaBr}_3:\text{Ce}$ .<sup>81</sup> If true, defect-related emission from pure bulk crystals of  $\text{Cs}_4\text{PbBr}_6$  will be beneficial in medical diagnostic applications like time-of-flight positron-emission tomography which rely more on time resolution along with light yield, and consequently, require fast scintillation decay, preferably in the sub-nanosecond timescale.

In conclusion, there are two opposing sets of thought, where one believes  $\text{CsPbBr}_3$  nanocrystals and inclusions, and the other believes defects in  $\text{Cs}_4\text{PbBr}_6$  to be the sole cause of green luminescence. Resolving this dichotomy is essential not just for scientific reasons, but is also necessary for successful practical applications which demand an answer to the question – are we growing  $\text{CsPbBr}_3$ ,  $\text{Cs}_4\text{PbBr}_6$  or a composite like dots-in-a-matrix?

## Epilogue

Koushik is grateful to have had many stimulating and enlightening conversations with Prof. Richard T. Williams on this



topic, and generally in the field of scintillators and radiation detectors. In addition to his scientific contributions, his kind mentorship will be sorely missed.

## Conflicts of interest

The author declares no competing financial interests.

## Acknowledgements

This work did not receive any specific grant from funding agencies in the public, commercial, or not-for-profit sectors. We acknowledge Dr Mahua Choudhury and Anastasia Jerman for organizing references.

## References

- Best Research Cell-Efficiency Chart, (<https://www.nrel.gov/pv/cell-efficiency.html>).
- A. K. Jena, A. Kulkarni and T. Miyasaka, *Chem. Rev.*, 2019, **119**, 3036–3103.
- X. Wang, T. Li, B. Xing, M. Faizan, K. Biswas and L. Zhang, *J. Phys. Chem. Lett.*, 2021, **12**, 10532–10550.
- J. R. Long, L. S. McCarty and R. H. Holm, *J. Am. Chem. Soc.*, 1996, **118**, 4603–4616.
- E. G. Tulskey and J. R. Long, *Chem. Mater.*, 2001, **13**, 1149–1166.
- K. Biswas, S. Lany and A. Zunger, *Appl. Phys. Lett.*, 2010, **96**, 201902.
- M. Cola, V. Massarotti, R. Riccardi and C. Sinistri, *Z. Naturforsch., A: Phys. Sci.*, 1971, **26**, 1328–1332.
- T. Udayabhaskararao, L. Houben, H. Cohen, M. Menahem, I. Pinkas, L. Avram, T. Wolf, A. Teitelboim, M. Leskes, O. Yaffe, D. Oron and M. Kazes, *Chem. Mater.*, 2018, **30**, 84–93.
- M. Liu, J. Zhao, Z. Luo, Z. Sun, N. Pan, H. Ding and X. Wang, *Chem. Mater.*, 2018, **30**, 5846–5852.
- I. Y. Kuznetsova, I. S. Kovaleva and V. A. Fedorov, *Russ. J. Inorg. Chem.*, 2001, **46**, 1730–1735.
- M. Rodová, J. Brožek, K. Knížek and K. Nitsch, *J. Therm. Anal. Calorim.*, 2003, **71**, 667–673.
- I. Dursun, M. De Bastiani, B. Turedi, B. Alamer, A. Shkurenko, J. Yin, A. M. El-Zohry, I. Gereige, A. AlSaggaf, O. F. Mohammed, M. Eddaoudi and O. M. Bakr, *ChemSusChem*, 2017, **10**, 3746–3749.
- H. P. Beck, G. Clicqué and H. Nau, *Z. Anorg. Allg. Chem.*, 1986, **536**, 35–44.
- D. Becker and H. P. Beck, *Z. Anorg. Allg. Chem.*, 2004, **630**, 1924–1932.
- B. Kang, C. M. Fang and K. Biswas, *J. Phys. D: Appl. Phys.*, 2016, **49**, 395103.
- Y. He, M. Petryk, Z. Liu, D. G. Chica, I. Hadar, C. Leak, W. Ke, I. Spanopoulos, W. Lin, D. Y. Chung, B. W. Wessels, Z. He and M. G. Kanatzidis, *Nat. Photonics*, 2021, **15**, 36–42.
- G. Eperon, G. Paternò, R. Sutton, A. Zampetti, A. Haghighirad, F. Cacialli and H. Snaith, *J. Mater. Chem. A*, 2015, **3**, 19688–19695.
- X. Zhang, M. E. Turiansky and C. G. Van de Walle, *Cell Rep. Phys. Sci.*, 2021, **2**, 100604.
- M. Rodova, J. Brozek, K. Knizek and K. Nitsch, *J. Therm. Anal. Calorim.*, 2003, **71**, 667–673.
- C. C. Stoumpos, C. D. Malliakas, J. A. Peters, Z. Liu, M. Sebastian, J. Im, T. C. Chasapis, A. C. Wibowo, D. Y. Chung, A. J. Freeman, B. W. Wessels and M. G. Kanatzidis, *Cryst. Growth Des.*, 2013, **13**, 2722–2727.
- M. Velázquez, A. Ferrier, S. Péchev, P. Gravereau, J.-P. Chaminade, X. Portier and R. Moncorgé, *J. Cryst. Growth*, 2008, **310**, 5458–5463.
- C. K. Moller, *On the structure of caesium hexahalogenoplumbates (ii)*, *Mater.-Fys. Medd.*, Mater.-Fys. Medd. K. Dan. Vidensk. Selsk, Munksgaard, København, 1960, vol. 32, pp. 1–13.
- B. Kang and K. Biswas, *J. Phys. Chem. Lett.*, 2018, **9**, 830–836.
- J. Yin, H. Yang, K. Song, A. M. El-Zohry, Y. Han, O. M. Bakr, J.-L. Brédas and O. F. Mohammed, *J. Phys. Chem. Lett.*, 2018, **9**, 5490–5495.
- M. Nikl, E. Mihokova, K. Nitsch, F. Somma, C. Giampaolo, G. P. Pazzi, P. Fabeni and S. Zazubovich, *Chem. Phys. Lett.*, 1999, **306**, 280–284.
- Z. Zhang, Y. Zhu, W. Wang, W. Zheng, R. Lin, X. Li, H. Zhang, D. Zhong and F. Huang, *Cryst. Growth Des.*, 2018, **18**, 6393–6398.
- M. Sebastian, J. A. Peters, C. C. Stoumpos, J. Im, S. S. Kostina, Z. Liu, M. G. Kanatzidis, A. J. Freeman and B. W. Wessels, *Phys. Rev. B: Condens. Matter Mater. Phys.*, 2015, **92**, 235210.
- Q. A. Akkerman, S. Park, E. Radicchi, F. Nunzi, E. Mosconi, F. De Angelis, R. Brescia, P. Rastogi, M. Prato and L. Manna, *Nano Lett.*, 2017, **17**, 1924–1930.
- J. Yin, Y. Zhang, A. Bruno, C. Soci, O. M. Bakr, J.-L. Brédas and O. F. Mohammed, *ACS Energy Lett.*, 2017, **2**, 2805–2811.
- G. Jin, D. Zhang, P. Pang, Z. Ye, T. Liu, G. Xing, J. Chen and D. Ma, *J. Mater. Chem. C*, 2021, **9**, 916–924.
- H. Yang, Y. Zhang, J. Pan, J. Yin, O. M. Bakr and O. F. Mohammed, *Chem. Mater.*, 2017, **29**, 8978–8982.
- X. Wei, J. Liu, H. Liu, X. Lei, H. Qian, H. Zeng, F. Meng and W. Deng, *Inorg. Chem.*, 2019, **58**, 10620–10624.
- J. Jiang, D. Wang, M. Wu, P. Peng, F.-F. Li, F. Liu, R. Jing, X. Ma, Y. Chao, Z. Xiao and Q. Jiang, *APL Mater.*, 2020, **8**, 071115.
- R. Bose, Y. Zheng, T. Guo, J. Yin, M. N. Hedhili, X. Zhou, J.-F. Veyan, I. Gereige, A. Al-Saggaf, Y. N. Gartstein, O. M. Bakr, O. F. Mohammed and A. V. Malko, *ACS Appl. Mater. Interfaces*, 2020, **12**, 35598–35605.
- L. N. Quan, R. Quintero-Bermudez, O. Voznyy, G. Walters, A. Jain, J. Z. Fan, X. Zheng, Z. Yang and E. H. Sargent, *Adv. Mater.*, 2017, **29**, 1605945.
- Z. Qin, S. Dai, V. G. Hadjiev, C. Wang, L. Xie, Y. Ni, C. Wu, G. Yang, S. Chen, L. Deng, Q. Yu, G. Feng, Z. M. Wang and J. Bao, *Chem. Mater.*, 2019, **31**, 9098–9104.



- 37 A. Ray, D. Maggioni, D. Baranov, Z. Dang, M. Prato, Q. A. Akkerman, L. Goldoni, E. Caneva, L. Manna and A. L. Abdelhady, *Chem. Mater.*, 2019, **31**, 7761–7769.
- 38 Y. Zhang, M. I. Saidaminov, I. Dursun, H. Yang, B. Murali, E. Alarousu, E. Yengel, B. A. Alshankiti, O. M. Bakr and O. F. Mohammed, *J. Phys. Chem. Lett.*, 2017, **8**, 961–965.
- 39 D. Chen, Z. Wan, X. Chen, Y. Yuan and J. Zhong, *J. Mater. Chem. C*, 2016, **4**, 10646–10653.
- 40 J.-H. Cha, H.-J. Lee, S. H. Kim, K. C. Ko, B. J. Suh, O. H. Han and D.-Y. Jung, *ACS Energy Lett.*, 2020, **5**, 2208–2216.
- 41 X. Chen, F. Zhang, Y. Ge, L. Shi, S. Huang, J. Tang, Z. Lv, L. Zhang, B. Zou and H. Zhong, *Adv. Funct. Mater.*, 2018, **28**, 1706567.
- 42 J. Xu, W. Huang, P. Li, D. R. Onken, C. Dun, Y. Guo, K. B. Ucer, C. Lu, H. Wang, S. M. Geyer, R. T. Williams and D. L. Carroll, *Adv. Mater.*, 2017, **29**, 1703703.
- 43 L. Wu, H. Hu, Y. Xu, S. Jiang, M. Chen, Q. Zhong, D. Yang, Q. Liu, Y. Zhao, B. Sun, Q. Zhang and Y. Yin, *Nano Lett.*, 2017, **17**, 5799–5804.
- 44 F. Palazon, C. Urso, L. De Trizio, Q. Akkerman, S. Marras, F. Locardi, I. Nelli, M. Ferretti, M. Prato and L. Manna, *ACS Energy Lett.*, 2017, **2**, 2445–2448.
- 45 C. de Weerd, J. Lin, L. Gomez, Y. Fujiwara, K. Suenaga and T. Gregorkiewicz, *J. Phys. Chem. C*, 2017, **121**, 19490–19496.
- 46 L. Yang, D. Li, C. Wang, W. Yao, H. Wang and K. Huang, *J. Nanopart. Res.*, 2017, **19**, 258.
- 47 F. Palazon, G. Almeida, Q. A. Akkerman, L. De Trizio, Z. Dang, M. Prato and L. Manna, *Chem. Mater.*, 2017, **29**, 4167–4171.
- 48 Y. Ling, L. Tan, X. Wang, Y. Zhou, Y. Xin, B. Ma, K. Hanson and H. Gao, *J. Phys. Chem. Lett.*, 2017, **8**, 3266–3271.
- 49 G. Hu, W. Qin, M. Liu, X. Ren, X. Wu, L. Yang and S. Yin, *J. Mater. Chem. C*, 2019, **7**, 4733–4739.
- 50 F. Cao, D. Yu, X. Xu, Z. Han and H. Zeng, *J. Phys. Chem. C*, 2021, **125**, 3–19.
- 51 L. Wang, H. Liu, Y. Zhang and O. F. Mohammed, *ACS Energy Lett.*, 2020, **5**, 87–99.
- 52 Q. A. Akkerman, A. L. Abdelhady and L. Manna, *J. Phys. Chem. Lett.*, 2018, **9**, 2326–2337.
- 53 N. Riesen, M. Lockrey, K. Badek and H. Riesen, *Nanoscale*, 2019, **11**, 3925–3932.
- 54 M. Shin, S.-W. Nam, A. Sadhanala, R. Shivanna, M. Anaya, A. Jiménez-Solano, H. Yoon, S. Jeon, S. D. Stranks, R. L. Z. Hoyer and B. Shin, *ACS Appl. Energy Mater.*, 2020, **3**, 192–199.
- 55 F. Cao, D. Yu, W. Ma, X. Xu, B. Cai, Y. M. Yang, S. Liu, L. He, Y. Ke, S. Lan, K.-L. Choy and H. Zeng, *ACS Nano*, 2020, **14**, 5183–5193.
- 56 U. Petralanda, G. Biffi, S. C. Boehme, D. Baranov, R. Krahne, L. Manna and I. Infante, *Nano Lett.*, 2021, **21**, 8619–8626.
- 57 J. Yin, J.-L. Brédas, O. M. Bakr and O. F. Mohammed, *Chem. Mater.*, 2020, **32**, 5036–5043.
- 58 R. Sun, N. Liu, W. Zheng, J. Zhang, N. Li, H. Lian, H. Liu and Y. Zhang, *Chem. Mater.*, 2021, **33**, 3721–3728.
- 59 J.-H. Yang, Q. Yuan and B. I. Yakobson, *J. Phys. Chem. C*, 2016, **120**, 24682–24687.
- 60 X. Liu, W. Xie, Y. Lu, X. Wang, S. Xu and J. Zhang, *J. Mater. Chem. C*, 2022, **10**, 762–767.
- 61 J. Zhang, A. Wang, L. Kong, L. Zhang and Z. Deng, *J. Alloys Compd.*, 2019, **797**, 1151–1156.
- 62 H. Zhang, Q. Liao, Y. Wu, J. Chen, Q. Gao and H. Fu, *Phys. Chem. Chem. Phys.*, 2017, **19**, 29092–29098.
- 63 S. Zou, C. Liu, R. Li, F. Jiang, X. Chen, Y. Liu and M. Hong, *Adv. Mater.*, 2019, **31**, 1900606.
- 64 X. Chen, D. Chen, J. Li, G. Fang, H. Sheng and J. Zhong, *Dalton Trans.*, 2018, **47**, 5670–5678.
- 65 S. Seth and A. Samanta, *J. Phys. Chem. Lett.*, 2017, **8**, 4461–4467.
- 66 S. Seth and A. Samanta, *J. Phys. Chem. Lett.*, 2018, **9**, 176–183.
- 67 M. I. Saidaminov, O. F. Mohammed and O. M. Bakr, *ACS Energy Lett.*, 2017, **2**, 889–896.
- 68 M. I. Saidaminov, J. Almutlaq, S. Sarmah, I. Dursun, A. A. Zhumeckenov, R. Begum, J. Pan, N. Cho, O. F. Mohammed and O. M. Bakr, *ACS Energy Lett.*, 2016, **1**, 840–845.
- 69 M. De Bastiani, I. Dursun, Y. Zhang, B. A. Alshankiti, X.-H. Miao, J. Yin, E. Yengel, E. Alarousu, B. Turedi, J. M. Almutlaq, M. I. Saidaminov, S. Mitra, I. Gereige, A. AlSaggaf, Y. Zhu, Y. Han, I. S. Roqan, J.-L. Bredas, O. F. Mohammed and O. M. Bakr, *Chem. Mater.*, 2017, **29**, 7108–7113.
- 70 R.-T. Liu, X.-P. Zhai, Z.-Y. Zhu, B. Sun, D.-W. Liu, B. Ma, Z.-Q. Zhang, C.-L. Sun, B.-L. Zhu, X.-D. Zhang, Q. Wang and H.-L. Zhang, *J. Phys. Chem. Lett.*, 2019, **10**, 6572–6577.
- 71 L. Yang, T. Wang, X. Yang, M. Zhang, C. Pi, J. Yu, D. Zhou, X. Yu, J. Qiu and X. Xu, *Opt. Express*, 2019, **27**, 31207–31216.
- 72 M. Hu, C. Ge, J. Yu and J. Feng, *J. Phys. Chem. C*, 2017, **121**, 27053–27058.
- 73 X. Wang, J. Yu, M. Hu, Y. Wu, L. Yang, W. Ye and X. Yu, *J. Lumin.*, 2020, **221**, 116986.
- 74 Y.-K. Jung, J. Calbo, J.-S. Park, L. D. Whalley, S. Kim and A. Walsh, *J. Mater. Chem. A*, 2019, **7**, 20254–20261.
- 75 D. Han, H. Shi, W. Ming, C. Zhou, B. Ma, B. Saparov, Y.-Z. Ma, S. Chen and M.-H. Du, *J. Mater. Chem. C*, 2018, **6**, 6398–6405.
- 76 Z. Ning, X. Gong, R. Comin, G. Walters, F. Fan, O. Voznyy, E. Yassitepe, A. Buin, S. Hoogland and E. H. Sargent, *Nature*, 2015, **523**, 324–328.
- 77 R. T. Williams, W. W. Wolszczak, X. Yan and D. L. Carroll, *ACS Nano*, 2020, **14**, 5161–5169.
- 78 M.-H. Du and F. A. Reboredo, *Opt. Mater.: X*, 2020, **8**, 100066.
- 79 Y. Kajino, S. Otake, T. Yamada, K. Kojima, T. Nakamura, A. Wakamiya, Y. Kanemitsu and Y. Yamada, *Phys. Rev. Mater.*, 2022, **6**, L043001.
- 80 K. S. Song and R. T. Williams, *Self-trapped excitons*, Springer, Berlin, New York, 1996.
- 81 E. V. D. van Loef, P. Dorenbos, C. W. E. van Eijk, K. Krämer and H. U. Güdel, *Appl. Phys. Lett.*, 2001, **79**, 1573–1575.

